

Critical fields of multilayered films of Al and Ge

T. W. Haywood* and D. G. Ast

Department of Materials Science and Engineering, Cornell University, Ithaca, New York 14853

(Received 5 December 1978; revised manuscript received 15 May 1978)

Films consisting of multiple alternating layers of Al and Ge were fabricated with variable layer spacing, and the superconducting properties measured as a function of the layer spacing. The critical temperatures followed the theory of Garland as formulated by Petitt and Silcox with $\beta = 0.26$ and $k = 20 \text{ \AA}$. The critical fields parallel to the layers varied as $(1-t)^{1/2}$ with extrapolated zero-temperature values similar to a single film with the thickness of one Al layer. The critical fields perpendicular to the layers showed a marked positive curvature with respect to temperature at high reduced temperatures. These findings are discussed. A theory by Gray and Schuller can be used to predict quite accurately the grain size in the layers from the degree of positive curvature, but this theory does not account for the lack of positive curvature in parallel fields.

I. INTRODUCTION

The superconducting properties of metallic, multilayered, thin films have been investigated to search for effects enhancing the critical temperature T_c ,¹⁻⁸ or the critical current.^{9,10} In the latter applications the individual layer thicknesses are typically of the order of the magnetic screening length⁹ λ_0 in order to maximize flux pinning. Most investigations into the possibility of resonance effects⁸ or excitonic superconductors³⁻⁵ were carried out on very thin evaporated or sputtered layers of the order of or below 100 \AA , with emphasis on T_c effects.

Even smaller layer spacings can be achieved by intercalating naturally layered structures.¹¹ A considerable amount of research has been carried out on their superconducting properties, especially of the critical magnetic field, which shows a positive curvature as a function of temperature.¹²⁻¹⁴ In order to determine if this effect were unique to intercalated compounds, we decided to investigate the critical magnetic fields of films composed of very thin, alternating layers of Al and Ge. The dependence of the critical fields on layer thickness, temperature, orientation, and number of layers was studied as part of a general program concerned with the superconducting properties of multilayered systems.

II. EXPERIMENTAL ARRANGEMENTS

Films of approximately 1-mm width and 9.5-mm length were deposited on a rotating, liquid-nitrogen-cooled substrate by alternately exposing the substrate to Al and Ge sources via a rotating shutter. Base pressure of the stainless steel, ion pumped, ultrahigh-vacuum (UHV) system was $< 1 \times 10^{-9}$ Torr but rose to $\sim 1 \times 10^{-6}$ Torr during operation of both electron-beam sources. The de-

position rates of both sources were held constant at $750 \text{ \AA}/\text{min}$. Layer thickness was determined by the shutter rotation period. The total thickness of the films was kept constant at about 1.5 \mu m but the thickness of Al and Ge layers was varied from 30 to 230 \AA , with both materials having about the same layer thickness. These layer thicknesses are average values and were determined with calibrated crystal-oscillator-thickness monitors mounted on either side of the substrate. In order to minimize oxidation effects and avoid a spurious superconductor-insulator interface, all films were started and terminated with a Ge layer. The finished films were removed quickly from the UHV system and the edges were scribed off the strip to be measured. Within 20 min after evaporation, the films were mounted and placed in a liquid-helium Dewar precooled to 77 K in order to minimize structural changes that might occur at room temperature.

The critical temperature (T_c) of the films was measured prior to placing the magnet in position. The temperature (T) was determined by measuring the He vapor pressure at the top of the Dewar. The critical temperature of the films was defined as the temperature at which their resistance was $\frac{1}{2}$ of their normal-state resistance at 4.2 K .

The critical fields were determined by a standard four-terminal resistance measurement. A constant current from 0.1 to $10 \text{ A}/\text{cm}^2$ mean density was applied parallel to the layers and the long axis of the specimen, while the external field perpendicular to the current was slowly raised to drive the film normal. H_{c2} was arbitrarily defined as the field which restored the films resistance to $\frac{1}{2}$ its normal value. For the conclusions of this paper, this choice is not critical since selection of any other point on the transition simply shifts the H_{c2} curve respective to T without substantially changing the curvature.

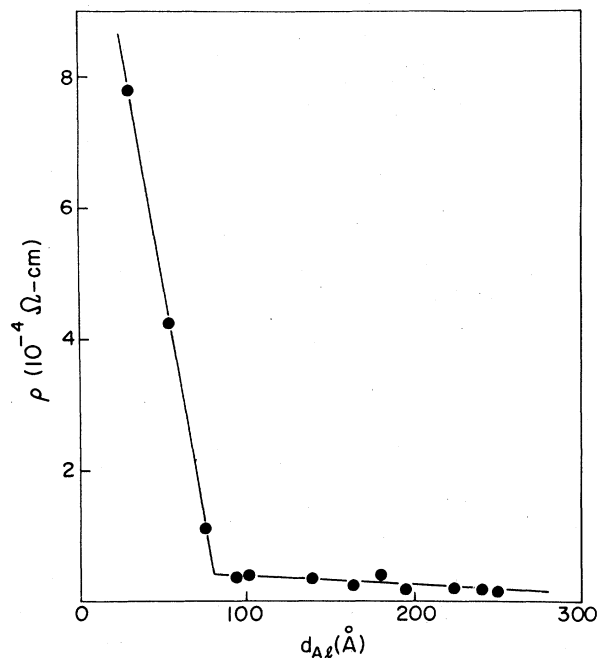


FIG. 1. Normal-state resistivity ρ as a function of d_{Al} .

The angular dependence of the critical fields was measured by rotating the magnet around the sample by means of a vernier control, which allowed setting the angle to within $\pm 0.05^\circ$. All measurements on the angular dependence of the critical fields were obtained with a current density of about 10 A/cm^2 .

III. RESULTS AND DISCUSSION

A. Film morphology

1. Normal-state resistivity

The normal-state resistivity parallel to the layers dropped about 10% between room temperature and 77°K . Between 77 and 4.2°K the normal-state resistivity was almost constant. The normal-state resistivity at 4.2°K as a function of layer thickness is shown in Fig. 1. It can be seen that a distinct change occurs at $d_{Al} \approx 80\text{--}90 \text{ \AA}$. Above this thickness the resistivity of the Al layers follows the prediction of boundary-scattering theory¹⁵

$$\sigma/\sigma_0 = 3d \ln(d/\Lambda_0)/4\Lambda_0, \quad (1)$$

where σ is the conductivity of a thin film of thickness d , σ_0 is the bulk conductivity, and Λ_0 is the bulk mean free path. For films with $d_{Al} > 90 \text{ \AA}$, Λ_0 was determined to be 1150 \AA . The abrupt change in the functional dependence of the resistivity at 80 \AA strongly suggests that the aluminum layers become discontinuous at this point, i.e., reach the

percolation threshold for conduction. Films with aluminum layer thickness less than 80 \AA still contain large two-dimensional clusters or islands of Al, as indicated by their low normal-state resistance ($< 10^{-3} \Omega\text{ cm}$). Films of zero layer thickness (Al and Ge codeposited on a rotating, liquid- N_2 -cooled substrate) had resistivities of order $10^{-1} \Omega\text{ cm}$ at 77°K and $1 \Omega\text{ cm}$ at 1.3°K , and did not become superconducting down to 1.3°K .

2. Grain size

In order to determine grain size, films were deposited on mica or NaCl substrates, floated off their substrate, and examined with transmission electron microscopy. The grain size varied approximately linearly with the Al layer thickness and could, within experimental error, be represented by

$$D = d_{Al} + 35, \quad (2)$$

where D is the grain diameter in \AA and d_{Al} is the thickness of the Al layers. In order to determine if grain size in layered films increased during deposition, a 140-layer Al-Ge film was ion milled from either side. TEM (transmission-electron-microscopy) analysis showed that the grain size was constant through the film.

3. Selective etching

The layered structure of the films was further confirmed by selective etching of the Al layers. The edge region of the films collapses as the etchant proceeds along the Al layers, leaving the Ge layers unsupported (see Fig. 2). In addition, the etching showed the presence of Al columns of $\sim 2 \mu\text{m}$ in diameter penetrating through the entire thickness of the film. The density of these defects was about 1.5×10^5 columns/ cm^2 , and was found to be independent of layer thickness. There is strong circumstantial evidence that these columnar defects are not present in freshly prepared films, but appear when the films are warmed up to room temperature. The column morphology is very similar to that of hillocks, which form in single evaporated Al films when cycled between liquid nitrogen or helium temperature and room temperature.¹⁹

B. Superconducting properties

1. Critical temperature

The critical temperature of freshly prepared films as a function of d_{Al} is shown in Fig. 3. The solid line was fitted using the theory of Garland *et al.*¹⁶ as formulated by Pettit and Silcox¹⁷



FIG. 2. Surface of a film selectively etched in NaOH as shown by the SEM (scanning electron microscope). Holes 2 μm in diameter were observed where Al columns penetrated the films, and collapsed edges where the NaOH selectively etched out the Al layers.

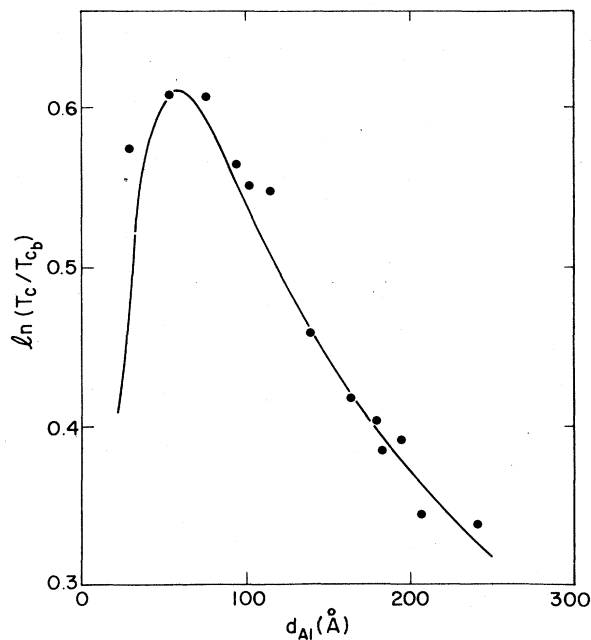


FIG. 3. Behavior of T_c as a function of d_{Al} . Line is the theory of Garland.

$$\ln \frac{T_c}{T_{c_b}} = \frac{-K/2D(1+\Lambda)}{A(1-\mu^*/2)\lambda - \mu^*} \times \frac{1+\lambda(1+K/D)}{A(1-\mu^*/2)\lambda(1+K/D)[1-\beta(K/D)/2] - \mu^*} \quad (3)$$

T_{c_b} is the bulk transition temperature; μ^* is the Coulomb pseudopotential (0.11); A is a constant which depends on crystal structure (0.90) and, in general, is reduced by the presence of lattice disorder; λ is the electron-phonon coupling constant such that $\lambda = \lambda_0(1+K/D)$ where λ_0 (0.41) is the bulk value of λ ; D is the grain diameter; K is a measure of the change of λ in the outer surface of the grain; and β is a measure of the lattice disorder

$$\beta = (\delta \ln A) / \delta \ln \langle \omega_{\text{ph}} \rangle, \quad (4)$$

where $\langle \omega_{\text{ph}} \rangle$ is the average phonon frequency. Note that Eq. (3) is a relation between T_c and D . Equation (2) was used to arrive at a relation between the experimentally measured variables d_{Al} and T_c . A fit of the data of this experiment yielded $\beta = 0.26$ and $K = 20 \text{ \AA}$, with T_{c_b} taken to be 1.18 K. Garland *et al.*¹⁶ measured $\beta = 0.52$ in granular Al films. In granular Al films in which the grains were coated with Al oxides, Pettit and Silcox¹⁷ find $\beta = 0.52$ and K of 10.5 \AA .

Finally, we observed that films stored at room temperature showed signs of structural changes. The transition broadened substantially along with a reduction in T_c in less than 24 h.¹⁸ The time scale of the decrease in T_c is compatible with the time scale of hillock growth in the Al layer, which is known to occur at room temperature.¹⁹

2. Critical fields

In all samples, the critical field perpendicular to the plane of the layers ($H_{c\perp}$) plotted versus T exhibited a marked positive curvature near T_c . However, $H_{c\perp}$ did not vary with temperature in a simple way (see Fig. 4) except at lower temperatures where $H_{c\perp}$ became linear in $T - T^*$, with $T^* < T_c$.

In all samples the critical field parallel to the layers ($H_{c\parallel}$) varied with temperature as $(1-t)^{1/2}$, where $t = T/T_c$. Therefore, under parallel fields, the films behaved essentially as a stack of noninteracting thin films, with individual thickness smaller than the coherence length ξ . Results for a typical film are shown in Fig. 4.

The values for the critical fields at zero temperature, $H_{c\perp}(0)$ and $H_{c\parallel}(0)$, can be grossly estimated by extrapolating the measured curves to $T = 0$. $H_{c\perp}(0)$ was determined by extrapolating the linear portion of $H_{c\perp}$ vs T . $H_{c\parallel}(0)$ was obtained by

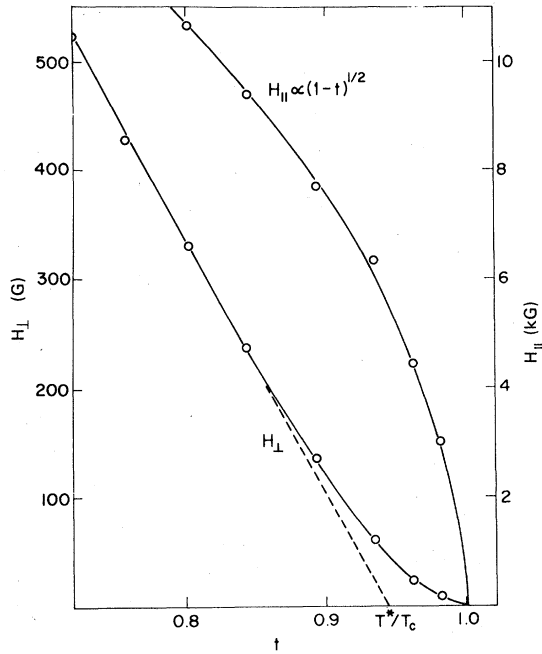


FIG. 4. H_c vs t for an Al-Ge layered film with each constituent layer approximately 140 Å.

assuming that the $(1-t)^{1/2}$ dependence held to $T=0$. The values thus obtained are represented in Fig. 5, where $[H_{c\perp}(0)]^{-1/2}$ and $[H_{c\parallel}(0)]^{-1/2}$ are plotted as a function of layer thickness. Figure 5 essentially represents a plot of the effective coherence length parallel and perpendicular to the plane of the layers since $H_{c\perp} \propto \xi_{\text{eff}}^{-2}$ and $H_{c\parallel} \propto \xi_{\parallel}^{-2}$.

The general trend of increasing $H_{c\parallel}(0)$ with decreasing d_{Al} is expected if the layers are acting as independent thin films. Also shown in Fig. 5 are the data of Tedrow and Meseervey²⁰ of $H_{c\parallel}$ of single thin films of Al. The agreement between the two sets of data indicates that the individual layers are indeed isolated by the field. Such an isolation is also expected from theory, since the penetration depth in the Ge layers is of the order of the layer width.²¹

The perpendicular field data have no straightforward interpretation.²² The ratio of $H_{c\parallel}(0)$ to $H_{c\perp}(0)$ was investigated by plotting $[H_{c\parallel}(0)/H_{c\perp}(0)]^{1/2}$ as a measure for the ratio of the effective coherence lengths $\xi_{\parallel}(0)/\xi_{\perp}(0)$ vs d_{Al} (see Fig. 6). This plot suggests that the ratio of the effective coherence length $\xi_{\parallel}(0)/\xi_{\perp}(0)$ varies approximately linearly with d_{Al} . Note, however, that in the effective-mass theory of layered superconductors²³ where $H_{c\parallel}(0) \propto \xi_{\perp} \xi_{\parallel}$ the ratio $[H_{c\parallel}(0)/H_{c\perp}(0)]^{1/2}$ would be interpreted as $[\xi_{\parallel}(0)/\xi_{\perp}(0)]^{1/2}$.

A peculiar feature of the data of Fig. 6 is the anomalous result that below a layer thickness of about 60 Å the perpendicular critical field at zero

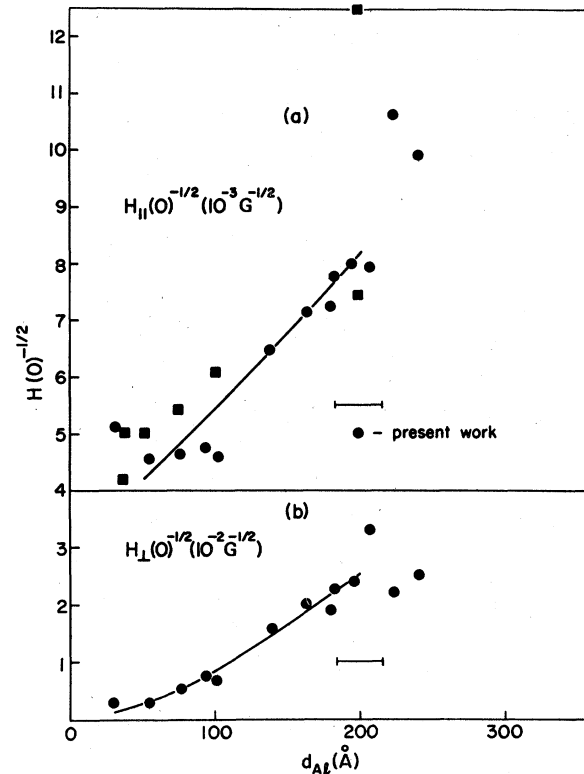


FIG. 5. General behavior of an effective coherence length defined as $[H(0)]^{-1/2} \propto \xi_{\text{eff}}(0)$ from extrapolated zero-temperature critical fields as a function of d_{Al} . Solid squares are data of Ref. 18.

temperature exceeds the parallel critical field at zero temperature. Although the extrapolation procedure used to find $H_{c\parallel}(0)$ in the thin-layer-thickness range is tenuous, despite agreement with the data of Tedrow and Meseervey, it is remarkable that the anomaly occurs at a layer thickness of 60 Å, i.e., coincides with the range of other anomalies, all of which suggest a breakup of Al layers.

3. Angular dependence of the critical fields

Figure 7 shows H_{c2} vs T as a function of the angle θ between the applied magnetic field and the plane of the layers. It can be seen that positive curvature is generally noticeable for $\theta \geq 2^\circ$. Some samples showed positive curvature for θ as small as 0.5° .

The angular dependence for small values of θ was investigated in more detail. At very small angles, the external field is parallel to the layers. The layers are then isolated magnetically, and the angular dependence expected is that of single thin films near the parallel orientation²⁴ $H_c(\theta) = H_{\text{TF}}(\theta)$, where

$$\left(\frac{H_{\text{TF}}(\theta)}{H_{c\parallel}} \cos \theta\right)^2 + \frac{H_{\text{TF}}(\theta)}{H_{c\perp}} \sin \theta = 1, \quad (5)$$

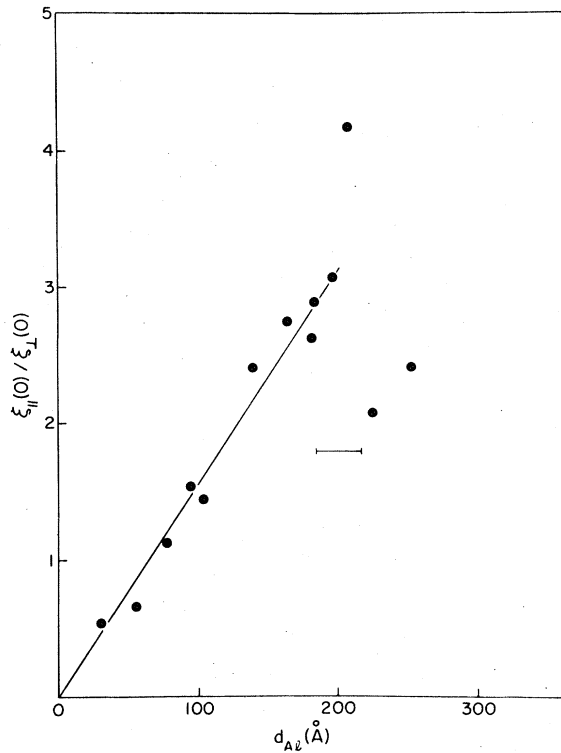


FIG. 6. Ratio of the two orientations in Fig. 5, $[H_{\perp}(0)]^{-1/2}/[H_{\parallel}(0)]^{-1/2}$.

and $H_{c\parallel}$ and $H_{c\perp}$ designate H_c parallel and perpendicular to the plane of the layers, respectively. Farther from the parallel condition, it was suspected that the samples would behave more as anisotropic superconductors, with a critical field dependence on angle as developed for layered structures with Josephson coupled layers²⁵: $H_c(\theta) = H_L(\theta)$, where

$$H_L(\theta) = H_{c\perp} / [\sin^2\theta + (H_{c\perp}/H_{c\parallel})^2 \cos^2\theta]^{1/2}. \quad (6)$$

To verify these expectations, the experimental results were compared with both theories. Figures 8 and 9 show the deviations between theory and experiment for various reduced temperatures by plotting

$$\Delta h_{TF} = (H_{exp} - H_{TF})/H_{exp}$$

and

$$(7)$$

$$\Delta h_L = (H_{exp} - H_L)/H_{exp}$$

vs T/T_c .

The Δ 's are normalized deviations between the experiment and thin film and layered theory, respectively, and H_{exp} is the experimentally measured critical field. A comparison between Figs. 8 and 9 shows that the predictions of the two theories only differ appreciably for $\theta < 3^\circ$ and $t < 0.9$. There is

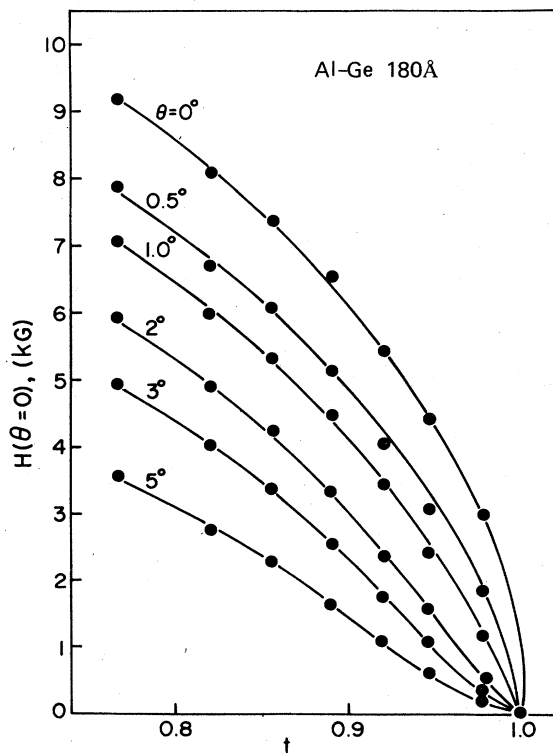


FIG. 7. Onset of positive curvature near T_c with the number of layers.

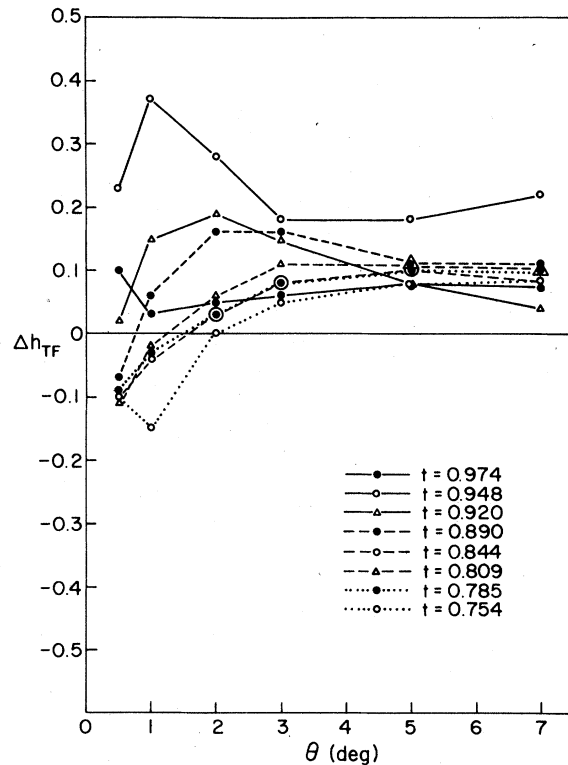


FIG. 8. $\Delta h_{TF} = (H_{TF} - H_{exp})/H_{exp}$ vs θ at various reduced temperatures for a typical sample.

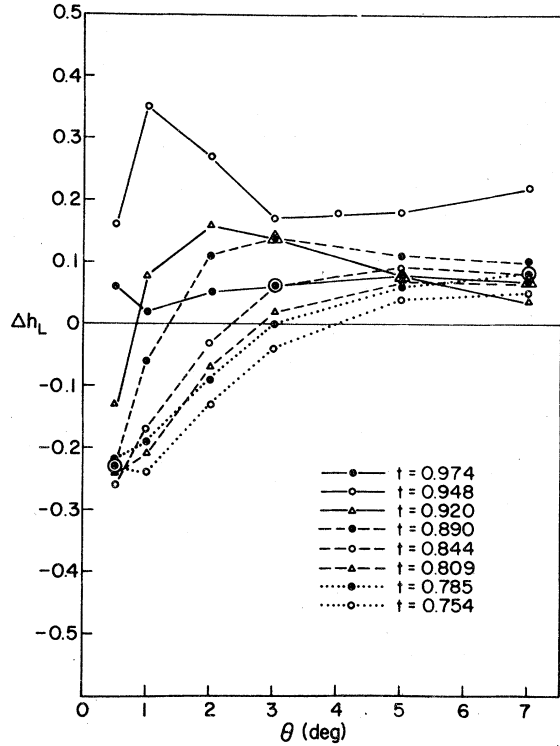


FIG. 9. $\Delta h_L = (H_L - H_{\text{exp}})/H_{\text{exp}}$ vs θ at various reduced temperatures for a typical sample.

considerable experimental scatter, but for $\theta < 3^\circ$ the experimental data gradually shift from agreement with the thin-film theory at $\theta = 0^\circ$ to agreement with layered theory at $\theta = 3^\circ$. Then H_{exp} appears to fall somewhat below both theories until about 10° , beyond which all three numbers H_{TF} , H_L , and H_{exp} are virtually identical. For $t > 0.9$ the prediction of the two theories are identical and differ from experiment as shown in Fig. 10, which shows Δh_{TF} of four different films at a fixed angle $\theta = 2^\circ$ as a function of reduced temperatures. It is seen that as $t \rightarrow 1$ the critical fields become much larger than predicted by either theory.

In order to determine the experimental error in $H_c(\theta)$ generated by an uncertainty of $\pm 0.05^\circ$ in the magnet setting (by far the dominating error in the experiment), it is necessary to calculate the error using one of the theories. Arbitrarily choosing the layered theory, one obtains from Eq. (5):

$$\frac{dH_c(\theta)}{d\theta} = 2H_{c\perp}(1 - \xi^2) \sin\theta \cos\theta \times (\sin^2\theta + \xi^2 \cos^2\theta)^{-3/2}, \quad (8)$$

where $\xi = H_{c\perp}/H_{c\parallel}$. For $\xi \ll 1$ and θ small, one may approximate

$$\frac{1}{H_c(\theta)} \frac{dH_c(\theta)}{d\theta} \approx \frac{\sin 2\theta}{\sin^2\theta + \xi^2 \cos^2\theta}. \quad (9)$$

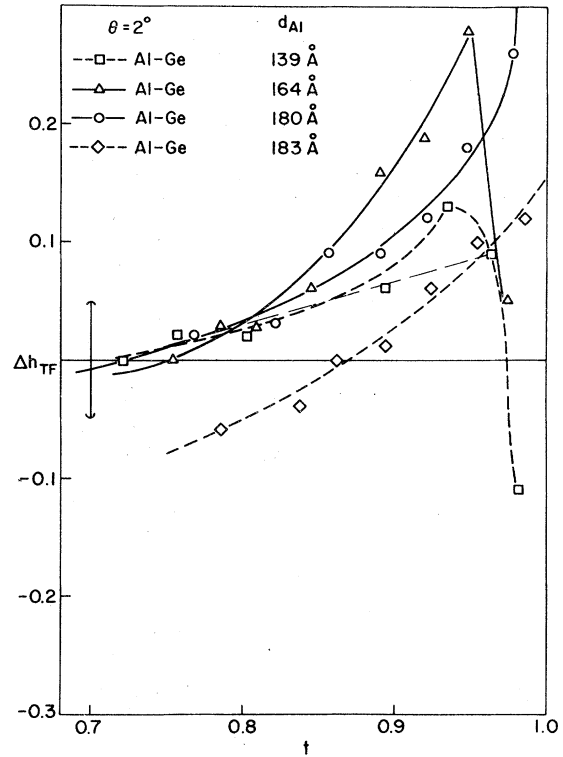


FIG. 10. $\Delta h_{\text{TF}} = (H_{\text{TF}} - H_{\text{exp}})/H_{\text{exp}}$ vs t for four samples at $\theta = 2^\circ$.

The error can be appreciable for small ξ and θ . Moreover, as ξ is very temperature dependent in these films, the degree of error involved is also temperature dependent for $\theta < 1^\circ$. The error bar shown in Fig. 10 reflects the maximum error (at $\xi = 0.002$) in the measurement at $\theta = 2^\circ$. The error in these measurements is substantial, but the data nevertheless support a trend toward thin-film behavior at $\theta = 0^\circ$ and layered behavior at $\theta = 3^\circ$ at lower reduced temperatures.

4. Variations of superconducting parameters with the total number of layers

The variations of the superconducting parameters with the number of layers were investigated in a series of films in which the Al layer thickness was kept constant at 160 \AA . The Al-Ge bilayer measured approximately 320 \AA .

The critical temperature and critical parallel field did not seem to depend on the size of the stack. T_c varied from 1.65 to 1.72°K with no obvious correlation with the number of layers. $H_{c\parallel}$ varied by no more than 10% from the mean at $T/T_c = 0.85$, indicating a fairly uniform layer thickness from film to film. $H_{c\parallel}$ showed no obvious correlation with the number of layers, in agreement with the idea that the layers were magnetically isolated

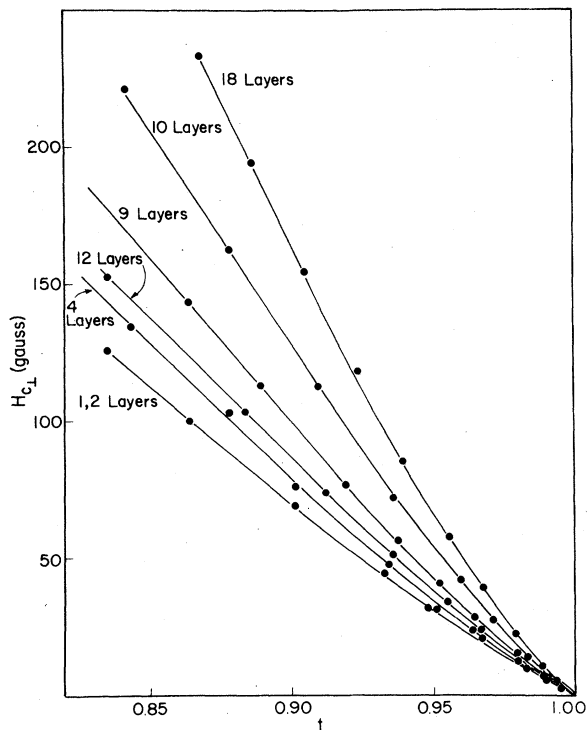


FIG. 11. $H_{c\perp}$ vs t as a function of the number of layers in films with $d_{Al} \approx 160 \text{ \AA}$.

by the field.

However, the perpendicular critical field did change markedly with the number of layers (see Fig. 11). It can be seen that both $H_{c\perp}$ and the degree of positive curvature tend to increase with the number of layers. Interestingly, even a single layer exhibits an overall positive curvature between $t=0.85$ and $t=1$ indicating that the overall positive curvature is probably not a result of layering per se. However, for one and two layers, the curvature does not remain positive at all values of t . Instead it is decidedly negative at $t \approx 1$, as can be seen more clearly in Fig. 12. $H_{c\perp}$ vs T becomes monotonic at three layers, and develops the standard type of curvature seen in all the film at four layers.

The increase in $H_{c\perp}$ with the number of layers is difficult to understand, unless one postulates that the structure of the film changes with the number of layers. For example, it is conceivable, that the surface roughness increases with the number of layers evaporated. In a rough surface, the current would flow mostly along planes which are not perpendicular to the applied field, since $H_{c\parallel} > H_{c\perp}$. Assuming that the first layer is perfectly flat, and assuming that the angular dependence of $H_{c\perp}$ follows

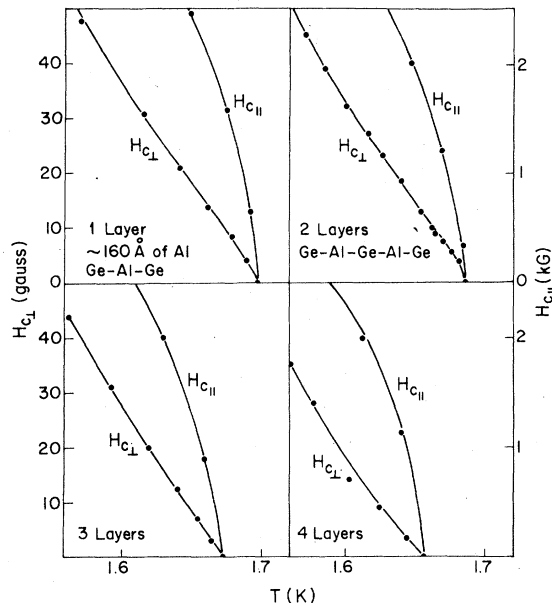


FIG. 12. H_c vs t as a function of the angle of the external field with the plane of the layers θ showing the onset of positive curvature. Specimen layers were 180 \AA thick.

thin-film theory,²⁴ the observed difference in $H_{c\perp}$ at $t=0.85$ between one layer and 18 layers implies that the effective superconducting path in the 18th layer occurs in a plane which is inclined at approximately 20° respective to the field or $\sim 70^\circ$ respective to the plane of the layers. This figure is highly improbable in view of the smooth appearance of our films when viewed in an interference microscope or in a scanning electron microscope. The observation that one and two layers behave virtually identically is compatible with the idea that some nonunderstood type of magnetic shielding partially screens interior layers from the applied fields. From such a model, no changes are expected until at least three aluminum layers are present.

C. Positive curvature of the critical field

A convenient measure of the degree of positive curvature is the ratio of the final slope ($-dH_c/dT$, $T < T^*$) to initial slope ($-dH_c/dT$, $T = T_c$), which we denote as γ . Figure 13 shows γ plotted as a function of aluminum layer thickness d_{Al} . It can be seen that γ increases uniformly with decreasing layer thickness down to about 80 \AA . Below 80 \AA an abrupt decrease in γ occurs which we associate with a breakup of the aluminum layers.

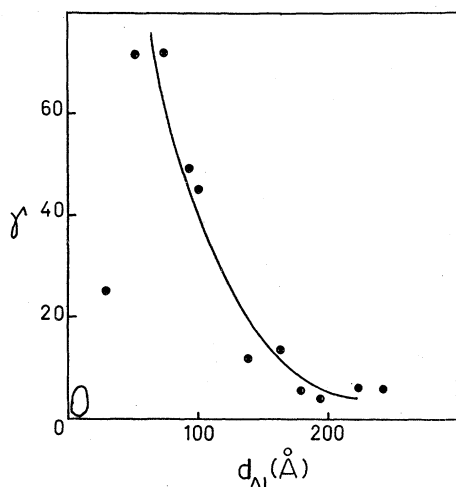


FIG. 13. Ratio $dH_{c\perp}/dT$ for $T < T^*$ to $dH_{c\perp}/dT$ for $T = T_c$, designated γ , as a function of Al layer thickness. Circled area near origin is from data of Refs. 11 and 25.

Remarkably, this breakup does not destroy the positive curvature. For purposes of comparison with intercalated materials, Fig. 13 also shows the general location of γ derived from $H_{c\perp}$ data from the intercalated materials investigated by Woollam *et al.*^{12,26} with no implication of significance to our system.

Associated with the positive curvature of $H_{c\perp}$ vs T is the intercept of the linear section, T^* . Figure 14 shows T^* as a function of d_{Al} . The data suggest the presence of two discontinuities in the plot, one at $d_{Al} = 100$ Å and one at $d_{Al} = 200$ Å, but in view of the experimental scatter a smooth interpretation is equally possible. In the discontinuity hypothesis the breaks would be associated with the loss of continuity in each of the two types of layer, Al and Ge. The slightly higher value of 100 Å could be due to experimental scatter, or to the fact that T^* may be more susceptible to layer continuity than say normal-state conductivity. Relatively little correlation between T^* and T_c was found other than a general trend of $t^* = T^*/T_c$ to increase with d_{Al} from about 0.85 below 100 Å to about 0.98 for $d_{Al} \approx 200$ Å.²²

At present there are several explanations that will allow for positive curvature of H_c vs T . Klemm *et al.*²⁷ and Toyota *et al.*¹⁴ have shown that a positive curvature of H_c vs T can be expected for layered superconductors with Josephson coupling between the layers. In both of these cases the positive curvature is much larger for the applied field parallel to the layers. Indeed Klemm *et al.* do not show a positive curvature for the perpendicular critical field. Entel and Peter²⁸ have shown that

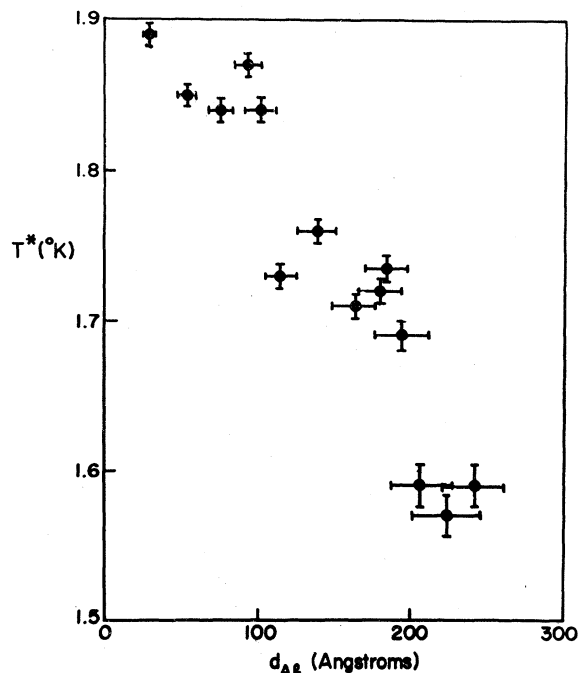


FIG. 14. Variation of the intercept of the linear portion of $H_{c\perp}$ vs T , T^* , as a function of aluminum layer thickness d_{Al} .

anisotropy in the Fermi surface can cause positive curvature in H_{c2} vs T , but in a polycrystalline material such an effect should not be limited to the perpendicular ($H_{c\perp}$) field. Gray and Schuller²⁹ proposed a model based on proximity-effect averaging in a granular film where there is a distribution of intrinsic critical temperatures among the grains. This theory should not be restricted to the perpendicular field configuration, but it conforms well enough to the data of this report that it will be discussed in more detail below. Deutscher and Dodds,³ who in granular Al films measure critical fields similar to ours, attribute their results to a change in dimensionality as the individual grains become isolated as T and $\xi(T)$ are reduced. And finally, flux flow or material inhomogeneities can cause positive curvature in H_c vs T . Section IIIC 1 discusses in detail the various types of positive curvature.

1. Material inhomogeneities

Two possible causes of anomalous positive curvature in H_c vs T data are compositional inhomogeneities of the layers and high- T_c filamentary shorts. The presence of inhomogeneities in the composition is improbable, as there are no complicating phases in the Al-Ge system to interfere with the definition of the layers, and the solubility of Ge in Al is below 0.2% at the maximum temp-

eratures reached by the substrate during deposition of the film. In addition, the existence of such inhomogeneities should be reflected in the critical field curves for all orientations of the external field, yet no anomaly is observed in the parallel critical field of these films (Fig. 4).

The parallel critical-field data indicate that if filamentary shorts are present they should be of the dimensions of the layer thickness in order for $H_{c\parallel}(0)$ to agree with published data on single thin films.²⁰ It is reasonable to expect the thinnest layer to short out the others as it would have a higher T_c and $H_{c\parallel}$. However, the slope of $H_{c\perp}$ vs T at T_c can be as much as two orders of magnitude lower than that of the linear portion of the curve (see Fig. 13). A high T_c , high $H_{c\parallel}$ filamentary short with diameter equal to the layer thickness must then have a perpendicular critical field 100 times smaller than the low T_c path in order to account for the positive curvature observed. From deposition-rate fluctuations, the layer thickness variation is expected to be only 10%–15%. It is, therefore, difficult to see how such a mechanism could account for the observed wide variation in $dH_{c\perp}/dT$ over the temperature range of the positive curvature.

2. Flux flow

The voltage one sees in any resistive measurement of H_{c2} during the transition can be at least partially due to flux flow in the superconductor. In most material a low current value will insure that the Lorentz force is too small to break the flux pins, so that the voltage is a clean measure of the amount of normal material in the film. However, perpendicular fields in thin aluminum films are so weakly pinned that even at the smallest experimentally feasible currents one cannot be certain that flux flow is absent. For this reason it is necessary to determine if flux flow can cause apparent positive curvature in a resistive measurement of H_{c2} .

The expected critical field curve for a Type-II superconductor near T_c is $H_{c2}(t) = \sqrt{2} \kappa H_c(1-t)$. This functional dependence should be an upper bound on the $H_{c2}(t)$ measured by resistivity as flux flow would reduce the measured H_{c2} at a given temperature. Any positive curvature should have the effect of returning the measured H_c vs t curve to the real H_{c2} vs t behavior. In order for the experimental curve to meet the real curve, its slope must somewhere have a magnitude greater than that of the real curve, and it must show negative curvature as it approaches the real curve smoothly.

In the high field region near H_{c2} , most theoretical pinning forces are of the form³¹

$$J_c = (sB_{c2}^n/\kappa^p)_b m'(1-b)l. \quad (10)$$

Here s is a constant function of the geometry of the microstructure, $b = B/B_{c2}$, κ is λ/ξ , and n' , m' , and l are exponents which depend on the specific pinning model used. If $\vec{J}_c \perp \vec{B}$, then

$$J_c \kappa^p / s = B_{c2}^n B^m (B_{c2} - B)^l, \quad (11)$$

where $n = n' - m' - l$ and $m = m' - l$. In standard resistive measurement of H_{c2} , where the voltage generated is actually due to flux flow, one measures not H_{c2} but some B defined by

$$B^m B_{c2}^n (B_{c2} - B)^l = C, \quad (12)$$

where $C = J_c \kappa^p / s$ is a constant.

The measured pinning force curve for the films of this study most closely follows the relation

$$F_p \propto b(1-b)^2. \quad (13)$$

This functional dependence is derived by Dew-Hughes³² for point pinning centers with the form

$$F_p = C B_{c2}^2 b(1-b)^2, \quad (14)$$

where C is a constant. One then obtains for the first derivative

$$\frac{dB}{dt} = \frac{(B_c + B)}{2B_c} \frac{dB_c}{dt}, \quad (15)$$

which states that the magnitude of the measured slope is always less than the magnitude of the slope of the actual B_{c2} vs t curve. Moreover, the minimum slope magnitude possible is $\frac{1}{2} |dB_c/dt|$. Therefore the slope may not vary by more than a factor of 2 in the region of the positive curvature. Figure 13 shows that the minimum change in this slope in the films of this study is approximately 5. The largest change was over a factor of 70.

Several other pinning models were investigated similarly.²² Those which predict a positive curvature to B vs t also require that $|dB/dt| < |dB_{c2}/dt|$, which is not acceptable if the positive curvature is to return the measured H_c to the intrinsic H_{c2} vs t line. If one does not stipulate that the curve return to the normal H_{c2} vs t behavior then one must accept values for the actual $H_{c1}(0)$ of the films which are much larger than large values already inferred from the measured data (see Fig. 5). For this reason, we conclude that flux pinning cannot account for the observed positive curvature in H_{c2} vs T .

3. Josephson coupling between layers

Toyota *et al.*¹⁴ have shown that Josephson coupling between layers as expected in the intercalated superconductors can cause a positive curvature to develop in the H_{c2} vs T curves for applied fields

both perpendicular and parallel to the layers. It is tempting to interpret the data of this study in terms of Josephson coupling between layers, but the thickness of the insulating Ge layers ($I > 30 \text{ \AA}$) places them outside the region where reasonable coupling should occur via tunneling ($I < 30 \text{ \AA}$). In the theory developed for Josephson-coupled systems, the positive curvature predicted in $H_{c\perp}$ is much less than that expected in $H_{c\parallel}$. That we observe no positive curvature in $H_{c\parallel}$ could be due to the large separation between the layers. As the penetration depth in the Ge is several millimeters,²¹ the parallel field should enter almost freely between the layers, and the Josephson coupling, being very sensitive to magnetic fields, should be extinguished. Thus any positive curvature which depended on the coupling would also be extinguished under parallel field conditions.

4. Proximity averaging among grains

Gray and Schuller²⁹ have shown that a distribution of T_c 's among the various grains of a film can result in a positive curvature because of a statistical narrowing of the T_c distribution through proximity effects among the grains. They define the width of the intrinsic distribution of T_c 's as $T^* - T_{cb}$, where T^* is the mean T_c of the film and T_{cb} is the bulk transition temperature (T_c of the largest grain). The width of the distribution of the local transition temperature is given by $T_c - T^*$. Assuming a Gaussian distribution of T_c 's, they find

$$T_c - T^* = (T^* - T_{cb})/N^{1/2}, \quad (16)$$

where N is the number of grains in a coherence volume.

One would not expect this theory to show anisotropy, that is, the effect of this distribution of T_c 's ought to be evident in $H_{c\parallel}$ as well as $H_{c\perp}$, contrary to the findings of this study.

Nevertheless, using this measure of the number of grains in a coherence volume and estimating the effective coherence length as the zero-temperature coherence length $\xi(0)$ as did Gray and Schuller, one can determine an average grain diameter $\langle D \rangle$, which agrees remarkably well with direct electron microscope measurement in our films. Estimating $\xi(0) = [(\frac{3}{2})^{1/2} \phi_0 / H_c(0)]^{1/2}$, one may obtain $\langle D \rangle$ as simply $\xi(0)/N^{1/3}$ for a three-dimensional sampling of grains by $\xi(0)$. In this study one expects the layers to be isolated by the Ge so that a two-dimensional sampling would be more normal, i.e., $\langle D \rangle \approx \xi(0)/N^{1/2}$. However, it was found that $\xi(0)/N^{1/3}$ predicted $\langle D \rangle$ correctly, perhaps indicating that the layers are coupled in some way. Figure 15 shows the results of the calculated $\langle D \rangle$ for each film of the study (solid

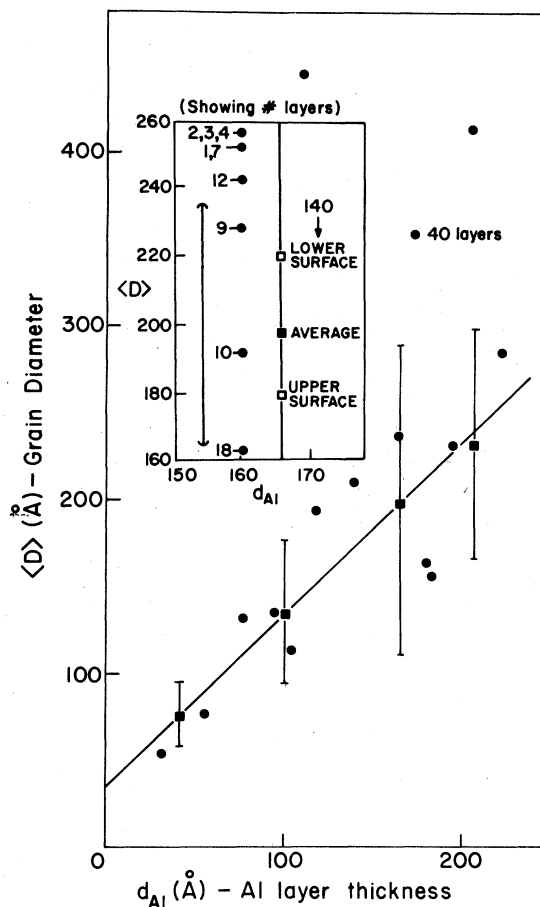


FIG. 15. Mean grain diameter vs d_{Al} . Solid circles are calculated from the degree of positive curvature using theory of Ref. 27. Straight line is a least-square fit to the solid circles. Solid squares are values measured in an electron microscope.

circles), assuming $\langle D \rangle = \xi(0)N^{1/3}$. The straight line through the data is a least-square fit to *only* the solid circles, neglecting the three points above 350 \AA . The solid squares are mean grain diameters as determined by electron microscopy. The fit to the line is remarkably good. Error bars on the solid squares are rms deviations on the measured distribution of grain diameters in the test films.

Similar calculations for the series of films where the number of layers was varied is shown in the inset in Fig. 15. Due to an increasing $H_{c\perp}(0)$, the general trend shows a reduction in computed grain size with increasing number of layers.

Error bars show the effect of the spread in T_c 's among the films which was not correlated with number of layers. However, electron microscope measurement of grain size on both the top and

bottom of a 140-layer film were not precise enough to confirm the decrease in computed grain size.

5. Dimensionality transition

Deutscher and Dodds³⁰ have observed a positive curvature in H_{c2} in Al films qualitatively similar to that of this study. Their films were also grown by electron-beam evaporation, but in an O_2 environment to produce dirty films. They cite evidence indicating that their films are layered. The critical field anisotropies of that study are similar to those of our films with extremely thin layers (30 Å). Their interpretation of the positive curvature observed is that a change in dimensionality occurs as T and $\xi(T)$ are reduced, so that at lower temperatures the grains become isolated. In their view, further evidence for the dimensionality change is the observation that the region of positive curvature starts at low temperatures for moderately dirty films and moves closer to T_c for dirtier films. Thus the grains begin to decouple at high temperature in the dirtier films.

Their approach is very adaptable to some of the results of this study: the crossover of $H_{c\perp}$ and $H_{c\parallel}$ at 60 Å at 0°K implied by Fig. 6 might be interpreted as a point of zero dimensionality, and the general shift of $t^* = T^*/T_c$ from low values (0.85) for thin Ge layers (30 Å) to high values (0.98) for thick Ge layers (200 Å) may indicate an increased decoupling with increased Ge content in the film. However, difficulties arise when one considers that the decoupling responsible for the positive curvature is the decoupling of grains in the plane of the layers. While 200 Å Ge layers would certainly facilitate decoupling of the Al layers, the layers should be very well defined. The grains in the 200 Å thick Al layers should be coupled much more strongly than those in the 30 Å layers. Furthermore, the linear portion of $H_{c\perp}$ vs T of this study indicates the presence of a stable configuration at temperatures much higher than would be required to isolate the grains; indeed, all of the films with $d_{Al} > 60$ Å had extrapolated $H_{c\parallel}(0) > H_{c\perp}(0)$ so that no zero dimensionality would occur at any temperature. For these reasons we doubt that the positive curvature of this study is solely a result of a change of dimensionality within the layers of the film.

IV. SUMMARY

Films consisting of multiple alternating layers of Al and Ge were fabricated with variable layer spacing, and the superconducting properties measured as a function of the layer spacing and num-

ber of layers. The critical field perpendicular to the plane of the layers shows a marked positive curvature with respect to temperature at high reduced temperatures; at lower reduced temperatures the curvature goes to zero. The critical fields parallel to the layers vary at $(1-t)^{1/2}$ and have extrapolated zero-temperature values similar to those of films with a total thickness equal to the thickness of one aluminum layer. Therefore, it is concluded that the layers are magnetically isolated by a field parallel to the layers so that each acts as an independent thin film. Positive curvature of H_c vs T is evident in all cases for fields oriented at angles of greater than 2° to the plane of the layers. The positive curvature in thinnest layers is so extreme that extrapolation to zero temperature predicts that the field perpendicular to the layer will equal that parallel to the layer for a layer thickness of 60 Å. This reflects the general trend that the positive curvature increases with decreasing layer thickness to about 60 Å, where it decreases rapidly as layer thickness is lowered.

A study of the positive curvature as a function of the number of layers shows that the positive curvature is partially present for even a single layer at lower reduced temperatures, showing that the layering is not responsible for this part of the curve. However, for $T \lesssim T_c$ there is a definite negative curvature for one and two layers, and the positive curvature does not extend smoothly to T_c until four layers are present. The degree of positive curvature does increase with increased number of layers even though electron microscopy analysis of grain size shows no significant difference between the top and bottom layers.

The positive curvature cannot be adequately explained by material inhomogeneities, filamentary shorts, or flux flow anomalies. Due to the thickness of the Ge layers it is not amenable to the layered superconductor theories based on Josephson coupling between the layers. A theory by Gray and Schuller³⁰ can be used to quite accurately predict grain size in the layers from the degree of positive curvature, but does not account for the lack of curvature anomaly in the parallel configuration. Finally, the proposal by Deutscher and Dodds³¹ of a reduction in dimensionality with reduced temperature is an intrinsically appealing qualitative explanation of the data, yet does not fully allow for the degree of coupling between Al grains within the layers that is believed present in this study. Neither does the linear portion of H_c vs T allow for a continuous reduction in dimensionality with T as is characteristic of their model.

There is evidence that the critical field perpendicular to the layers is affected by the number of

layers, even though the aluminum layers are relatively well separated by Ge. Whether the layers interact via weak-link shorts across the Ge, or by dc transformer-type coupling via the flux lines, or by some sort of magnetic shielding is not presently known.

ACKNOWLEDGMENTS

It is our pleasure to acknowledge the advice and technical aid of E. J. Kramer, J. E. Clemans, Wilson Yetter, and Helmut Föll during this study, and the financial support by the Air Force through Grant No. F44620-74-C-0019.

-
- *Present address: Physics Dept., University of North Carolina at Wilmington, Wilmington, N. C. 28401.
- ¹Morrell H. Cohen and D. H. Douglass, Jr., *Phys. Rev. Lett.* **19**, 118 (1967).
 - ²D. L. Miller, M. Strongin, and O. F. Kammerer, *Phys. Rev. B* **13**, 4834 (1976).
 - ³M. Strongin *et al.*, *Phys. Rev. Lett.* **21**, 1320 (1968).
 - ⁴V. L. Ginzburg, *Sov. Phys. Usp.* **13**, 335 (1970).
 - ⁵A. Fontaine and E. Meunier, *Phys. Kondens. Mater.* **14**, 119 (1972).
 - ⁶David Allender, James Bray, and John Bardeen, *Phys. Rev. B* **7**, 1020 (1973).
 - ⁷C. C. Tsuei and W. L. Johnson, *Phys. Rev. B* **9**, 4742 (1974).
 - ⁸K. A. Osipov, A. F. Orlov, V. P. Duritriev, and A. K. Milai, *Sov. Phys. Solid State* **19** (8), 1304 (1977).
 - ⁹H. Raffy, J. C. Renard and E. Guyon, *Solid State Commun.* **11**, 1659 (1972); **14**, 427 (1974); **14**, 431 (1974).
 - ¹⁰M. Kubic and L. Dobrosavljevic, *Phys. Status Solidi B* **75**, 677 (1976).
 - ¹¹F. R. Gamble, F. J. D. Salvo, R. A. Klemm, and T. H. Geballe, *Science* **168**, 568 (1970).
 - ¹²John A. Woollam and Robert B. Somoano, *Phys. Rev. B* **13**, 3854 (1976).
 - ¹³L. N. Bulaevskii and A. A. Guseinov, *JETP Lett.* **19**, 382 (1974).
 - ¹⁴N. Toyota *et al.*, *J. Low Temp. Phys.* **25**, 485 (1976).
 - ¹⁵J. M. Ziman, *Electrons and Phonons* (Oxford U.P., London, 1960, 1955), p. 468.
 - ¹⁶J. W. Garland, K. H. Bennemann, and F. M. Mueller, *Phys. Rev. Lett.* **21**, 1315 (1968).
 - ¹⁷Richard B. Pettit and J. Silcox, *Phys. Rev. B* **13**, 2865 (1976).
 - ¹⁸T. W. Haywood and D. G. Ast, Materials Science Center Report No. 2956, Cornell University (1977) (unpublished).
 - ¹⁹P. Chaudhari, *J. Appl. Phys.* **45**, 4339 (1974).
 - ²⁰P. M. Tedrow and R. Meservey, *Phys. Rev. B* **8**, 5098 (1973).
 - ²¹P. G. DeGennes, *Superconductivity of Metals and Alloys* (Benjamin, New York, 1966), p. 243.
 - ²²T. W. Haywood and D. G. Ast, Materials Science Center Report No. 2718, Cornell University (1976) (unpublished).
 - ²³W. E. Lawrence and S. Doniach, in *Proceedings of the International Conference on Low Temperature Physics* (Academic, Japan, Kyoto, 1971), p. 361.
 - ²⁴M. Tinkham, *Phys. Lett.* **9**, 217 (1964).
 - ²⁵L. Dobrosavljevic, *Phys. Status Solidi B* **55**, 773 (1973).
 - ²⁶John A. Woollam, Robert B. Somoano, and Paul O'Conner, *Phys. Rev. Lett.* **32**, 712 (1974).
 - ²⁷R. A. Klemm, A. Luther, and M. R. Beasley, *Phys. Rev. B* **12**, 877 (1975).
 - ²⁸P. Entel and M. Peter, *J. Low Temp. Phys.* **22**, 613 (1976).
 - ²⁹K. E. Gray and I. Schuller, *J. Low Temp. Phys.* **28**, 75 (1977).
 - ³⁰G. Deutscher and S. A. Dodds, *Phys. Rev. B* **16**, 3936 (1977).
 - ³¹A. M. Campbell and J. E. Evetts, *Adv. Phys.* **21**, 199 (1972).
 - ³²D. Dew-Hughes, *Philos. Mag.* **30**, 293 (1974).



FIG. 2. Surface of a film selectively etched in NaOH as shown by the SEM (scanning electron microscope). Holes $2\ \mu\text{m}$ in diameter were observed where Al columns penetrated the films, and collapsed edges where the NaOH selectively etched out the Al layers.